

Palladium(II) and Palladium(0) Complexes of Pyridylthioether-Based Metallodendrimers. Synthesis, Characterization, and Mechanistic Study of the Influence of Wedge Size on Allyl Amination

Luciano Canovese,* Gavino Chessa,* Claudio Santo, Fabiano Visentin, and Paolo Uguagliati

Dipartimento di Chimica, Università Ca' Foscari di Venezia, Dorsoduro 2137, I-30123, Venezia, Italy

Received May 14, 2002

Pd(II) allyl and Pd(0) fumaronitrile complexes bearing pyridyl-dithioether-based dendrimers as ancillary ligands have been synthesized and fully characterized by means of NMR spectrometry, elemental analysis, and MALDI-TOF technique. The fluxional behavior of the species was investigated by studying the ^1H NMR spectra recorded in CD_2Cl_2 at variable temperature and interpreted on the basis of a windshield-wiper motion of the dendritic wings which alternatively coordinate at the metal core. The reactivity of piperidine on the Pd(II) allyl substrates to give the allylamine derivative and the corresponding Pd(0) fumaronitrile species was also studied. The second-order rate constants k_2 and the equilibrium constants K_E relating to piperidine attack on the allyl fragment and to the concomitant displacement of the dendrimer ligand by piperidine, respectively, were determined and discussed taking into account the increasing dendritic size. Surprisingly, no macroscopic effects are observed on going from the model molecule to the second-generation dendritic substrates, and only with the third generation dendritic wedge complex are remarkable variations in the rate and equilibrium constants observed. We therefore advance the hypothesis that a sudden rearrangement at this stage occurs in solution. Such a rearrangement would induce an increase of steric hindrance at the allyl fragment and a concomitant distortion of the ligand in the environment of the metal core, thereby justifying the decrease of k_2 and the increase of K_E values.

Introduction

Metallodendrimers are emerging as efficient and recyclable catalysts in many chemical reactions.^{1,2} Generally, metal centers involved in chemical reactions are placed either at the periphery or within the dendrimers.

Numerous studies in this area indicate that the dendritic framework exerts a considerable influence on the properties of the metal center. In particular, when the active site is located at the core, the dendritic superstructure around it can provide a shielding which generates a microenvironment reminiscent of those found in biological systems.^{3,4}

Among the functional dendrimers bearing catalytic pockets that mimic enzymes the "dendrzymes" reported by Brunner are noteworthy.⁵ Catalytic studies carried out on those systems showed a modest but favorable effect of the dendritic branching on the properties of the active site.

Extension of this concept to more elaborated structures^{6–9} provided significant insight into structure–activity effects. For example, Chow and Mak⁷ performed a detailed mechanistic study of the copper-catalyzed Diels–Alder reaction. Their results led to the conclusion that steric hindrance of the dendritic shell is a key factor. As a matter of fact, on going from the second to the third generation, the catalytic activity dropped while the selectivity increased slightly.

A similar effect was also observed by Seebach⁹ on studying the Ti-catalyzed enantioselective nucleophilic addition of Et_2Zn to benzaldehyde using dendrimers with TADDOL cores. Consequently, to optimize the properties of the catalyst, the dendritic systems should contain tailored microenvironments and even structural features promoting interactions between the active site and the reactants. However, the conformational behavior of dendrimers and its connection with the site present in the core is still a source of intriguing dispute,⁷ and further studies ought to be carried out in order to elucidate the influence of branched units on the reactivity of the metal core.¹⁰

* Corresponding authors. E-mail: cano@unive.it and chessa@unive.it.

(1) (a) Astruc, D.; Chardac, F. *Chem. Rev.* **2001**, *101*, 2991. (b) Twyman, L. J.; King, A. S. H.; Martin, I. K. *Chem. Soc. Rev.* **2002**, *31*, 69.

(2) Oosterom G. E.; Reek J. N. H.; Kamer P. C. J.; van Leeuwen P. W. N. M. *Angew. Chem., Int. Ed.* **2001**, *40*, 1828.

(3) Smith, D. K.; Diederich, F. *Chem. Eur. J.* **1998**, *4*, 1353.

(4) Hetch, S.; Fréchet, J. M. J. *Angew. Chem., Int. Ed.* **2001**, *40*, 74.

(5) Brunner, H. *J. Organomet. Chem.* **1995**, *500*, 39.

(6) Bolm, C.; Derrien, N.; Sarger, A. *Synlett.* **1966**, 387.

(7) Chow, H. F.; Mak, C. C. *J. Org. Chem.* **1997**, *62*, 5116.

(8) Yamago, S.; Furukuwa, M.; Azuma, A.; Yoshida, J. I. *Tetrahedron Lett.* **1998**, *39*, 3783.

(9) Rheiner, P. B.; Seebach, D. *Chem. Eur. J.* **1999**, *5*, 3221.

In this respect we chose to investigate the reactivity and the solution behavior of palladium(II) allyl complexes bearing dendritic wedges as ancillary ligands. Pd(II) allyl complexes have been systematically investigated as substrates in the reaction involving the nucleophilic attack by amines at the coordinated allyl ligand. In particular we investigated in depth the allylic amination of palladium allyl complexes bearing pyridyl-imines and pyridyl-thioethers as ancillary ligands. The ensuing wealth of available information allows a useful comparison with the results of the present work.¹¹ Moreover, since the accepted reaction mechanism of allyl amination in these systems consists of a fast equilibrium displacement of the ancillary ligand by the reacting amine parallel to nucleophilic attack of the amine itself to the coordinated allyl fragment (vide infra), information on both thermodynamic and kinetic issues could be gathered. In other words, the magnitude of the displacement equilibrium constants and of the bimolecular rate constants can be analyzed as a function of the increasing bulkiness of the dendritic wedges, thereby providing clear-cut information on the accessibility and on the consequent reactivity of the metal core.

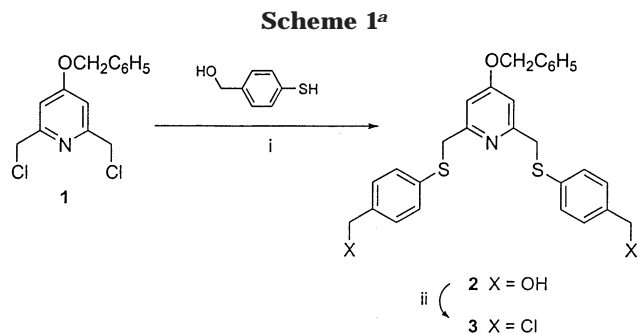
Recently¹² we reported on the synthesis of a series of dendritic pyridyl ligands, **7–9**, and the corresponding Pd(II) complexes. We report herein on mechanistic studies on the reactivity of the η^3 -allyl complexes containing such ligands toward amination with piperidine.

Results and Discussion

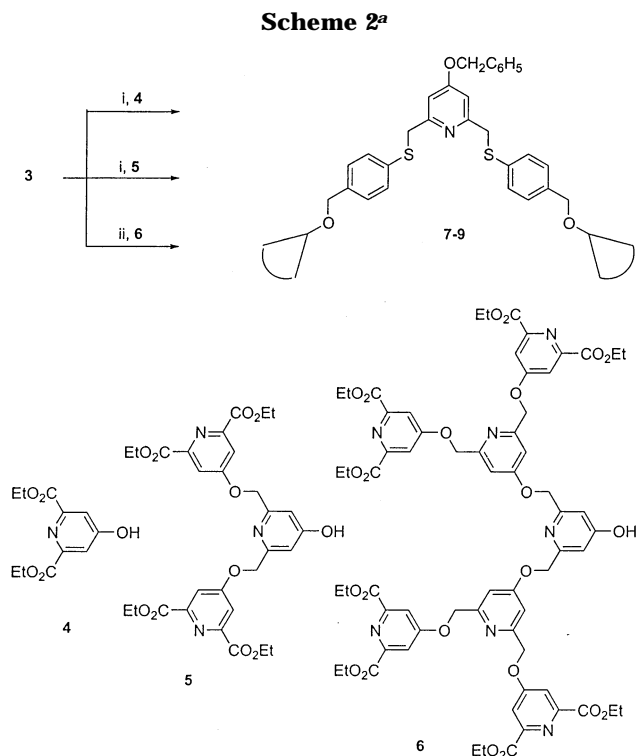
Synthesis of Dendritic Ligands. The dendritic ligands used in this study were designed for the incorporation of palladium into a specific binding site within the dendrimeric structure.¹²

The synthetic strategy leading to dendritic wedges **7–9** consists of preparing the building block **3** (Scheme 1) and coupling it with the known pyridine-based dendritic fragments **4–6**² (Scheme 2) to form ether linkages. The key intermediate **3** was synthesized from 4-benzyloxy-2,6-bis(chloromethyl)pyridine, **1**,^{13,14} as depicted in Scheme 1.

The introduction of the thioether functions was accomplished in 84% yield by reacting the dichloride **1** with 4-mercaptobenzyl alcohol¹⁵ in DMF in the presence



^a Reagents and conditions: (i) K_2CO_3 , 18-crown-6, DMF, 45 °C, 24 h; (ii) $SOCl_2$, 50 °C, 4 h.



^a Reagents and conditions: (i) K_2CO_3 , DMF, 70 °C, 24 h; (ii) K_2CO_3 , DMF, 60 °C, 48 h.

of K_2CO_3 and 18-crown-6 at 45 °C. The dihydroxymethyl derivative **2** was then converted to the corresponding dichloride **3** by treatment with $SOCl_2$ at 50 °C. After chromatographic purification, the building block **3** was obtained in 82% yield. Combination of 2 equiv of diethyl chelidamate **4** with the pyridylthioether-type ligand **3** under Williamson etherification conditions using K_2CO_3 as the base and DMF as the solvent gave the dendritic wedge SNS(**1**) (**7**) in 92% yield.

Similarly, coupling of the higher generation polypyridine dendritic fragments **5** and **6** with **3** provided the dendritic wedges SNS(**2**) (**8**) and SNS(**3**) (**9**) in 85% and 82%, respectively.

Dendritic wedges **7–9** were fully characterized by IR, ¹H and ¹³C NMR spectroscopy, MALDI-TOF mass spectrometry, and elemental analysis.

In general, the ¹H NMR spectra of the dendritic ligands **7–9** show signals attributable to aliphatic methylene, benzylic, and aromatic protons introduced

(10) Bosman, A. W.; Janssen, H. M.; Meijer, E. W. *Chem. Rev.* **1999**, *99*, 1665.

(11) (a) Crociani, B.; Antonaroli, S.; Di Bianca, F.; Canovese, L.; Visentin, F.; Uguagliati, P. *J. Chem. Soc., Dalton Trans.* **1994**, 1145. (b) Canovese, L.; Visentin, F.; Uguagliati, P.; Di Bianca, F.; Antonaroli, S.; Crociani, B. *J. Chem. Soc., Dalton Trans.* **1994**, 3113. (c) Canovese, L.; Uguagliati, P.; Visentin, F.; Crociani, B.; Di Bianca, F. *Inorg. Chim. Acta* **1995**, *235*, 45. (d) Crociani, B.; Antonaroli, S.; Paci, M.; Di Bianca, F.; Canovese, L. *Organometallics* **1997**, *16*, 384. (e) Canovese, L.; Visentin, F.; Uguagliati, P.; Chessa, G.; Lucchini, L.; Bandoli, G. *Inorg. Chim. Acta* **1998**, *275–276*, 385. (f) Canovese, L.; Visentin, F.; Uguagliati, P.; Bandoli, G. *Inorg. Chim. Acta* **1998**, *277*, 247–252. (g) Canovese, L.; Visentin, F.; Uguagliati, P.; Chessa, G.; Pesce, A. *J. Organomet. Chem.* **1998**, *566*, 61. (h) Canovese, L.; Visentin, F.; Chessa, G.; Niero, A.; Uguagliati, P. *Inorg. Chim. Acta* **1999**, *293*, 44. (i) Canovese, L.; Visentin, F.; Santo, C.; Chessa, G.; Uguagliati, P. *Polyhedron* **2001**, *20*. (j) Canovese, L.; Visentin, F.; Chessa, G.; Gardenal, G.; Uguagliati, P. *J. Organomet. Chem.* **2001**, *622*, 155.

(12) Chessa, G.; Scriveranti, A.; Canovese, L.; Visentin, F.; Uguagliati, P. *Chem. Commun.* **1999**, 959.

(13) Chessa, G.; Scriveranti, A. *J. Chem. Soc., Perkin Trans. 1* **1996**, 307.

(14) Chessa, G.; Scriveranti, A. *J. Heterocycl. Chem.* **1997**, 1851.

(15) Gricen R.; L. N. Owen, *J. Chem. Soc.* **1963**, 1947.

by the pyridylthioether ligand in addition to the expected patterns arising from the pyridyl fragments **4–6**.¹³

Also MALDI-TOF analysis of compounds **7–9** gave mass spectra, characterized by the presence of $[M + H]^+$, $[M + Na]^+$, and $[M + K]^+$ ions for all the samples under study. The m/z values of the observed ions are in agreement with related theoretical average masses (percent error of measured mass < 0.5%).

Synthesis of Palladium(II) Allyl Complexes. Addition at RT of 2,6-bis(phenylthiomethylpyridine) (SNS(**0**))^{11j} as reference compound and of the appropriate dendritic ligand SNS(**1**), SNS(**2**), and SNS(**3**) to the dimeric species $[Pd_2(\mu-Cl)_2(\eta^3-C_3H_5)_2]$ ¹⁶ or $[Pd_2(\mu-Cl)_2(\eta^3-1,1-(CH_3)_2C_3H_3)_2]$ ¹⁷ in CH_2Cl_2 yields the required allyl complex upon chloride abstraction with a stoichiometric amount of $AgSO_3CF_3$.

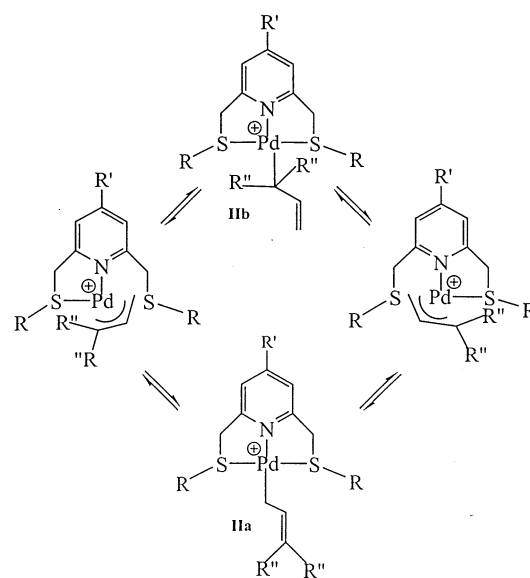
The complexes were obtained in 76%, 75%, 59%, and 86% yield in the cases of $[Pd(\eta^3-C_3H_5)SNS(\mathbf{0})]SO_3CF_3$, $[Pd(\eta^3-C_3H_5)SNS(\mathbf{1})]SO_3CF_3$, $[Pd(\eta^3-C_3H_5)SNS(\mathbf{2})]SO_3CF_3$, and $[Pd(\eta^3-C_3H_5)SNS(\mathbf{3})]SO_3CF_3$ and 73%, 73%, 72%, and 88% yield in the cases of $[Pd(\eta^3-1,1-(CH_3)_2C_3H_3)SNS(\mathbf{0})]SO_3CF_3$, $[Pd(\eta^3-1,1-(CH_3)_2C_3H_3)SNS(\mathbf{1})]SO_3CF_3$, $[Pd(\eta^3-1,1-(CH_3)_2C_3H_3)SNS(\mathbf{2})]SO_3CF_3$, and $[Pd(\eta^3-1,1-(CH_3)_2C_3H_3)SNS(\mathbf{3})]$, respectively.

¹H NMR spectrometry provides a timely check on the complex formation since coordinated allyl proton signals are easily detectable and selected significant signals of the free ligand shift downfield upon coordination. The complexes were also characterized by elemental analysis and MALDI-TOF technique. In the latter case the mass spectra are characterized by the presence of ions corresponding to $[SNS Pd]^+$ and $[SNS Pd allyl]^+$ ionic species.

Solution Behavior of Palladium(II) Allyl Complexes. Selected ¹H and ¹³C NMR data for the new complexes are reported in the Experimental Section.

It has been shown^{11f} that in the solid state palladium(II) allyl complexes bearing potentially terdentate pyridyl-dithioether SNS ligands are tetracoordinated species with the allyl fragment η^3 -coordinated and the SNS moiety acting as bidentate; consequently the complexes $[Pd(\eta^3-C_3H_5)SNS(\mathbf{0})]SO_3CF_3$, $[Pd(\eta^3-C_3H_5)SNS(\mathbf{1})]SO_3CF_3$, $[Pd(\eta^3-C_3H_5)SNS(\mathbf{2})]SO_3CF_3$, and $[Pd(\eta^3-C_3H_5)SNS(\mathbf{3})]SO_3CF_3$ are expected to exist as couples of diastereoisomers deriving from the mutual position of the allyl H² and the coordinated sulfur substituent R, which may be on the same or on the opposite side of the main coordination plane. In the case of the complexes $[Pd(\eta^3-1,1-(CH_3)_2C_3H_3)SNS(\mathbf{0})]SO_3CF_3$, $[Pd(\eta^3-1,1-(CH_3)_2C_3H_3)SNS(\mathbf{1})]SO_3CF_3$, $[Pd(\eta^3-1,1-(CH_3)_2C_3H_3)SNS(\mathbf{2})]SO_3CF_3$, and $[Pd(\eta^3-1,1-(CH_3)_2C_3H_3)SNS(\mathbf{3})]SO_3CF_3$ four distinct isomers should be present since, besides the above-mentioned species, the substituted allyl terminal carbon can be either *cis* or *trans* to the central coordinating pyridyl nitrogen atom (the existing enantiomers go undetected under our experimental conditions). However, the RT ¹H NMR spectral data strongly suggest the presence in solution of symmetric structures in which no differences between coordinated and uncoordinated SNS branches can be detected and the allyl

Scheme 3



R = C₆H₅; DENDRITIC WEDGES

R' = H; OCH₂C₆H₅

R'' = H; Me

protons give rise to slightly broadened AX₄ or AX₂ structures in the case of unsubstituted or substituted allyl fragment, respectively. Owing to the most favorable signal ratio, we will discuss in this section only the solution behavior of $[Pd(\eta^3-C_3H_5)SNS(\mathbf{0})]SO_3CF_3$ and $[Pd(\eta^3-1,1-(CH_3)_2C_3H_3)SNS(\mathbf{0})]SO_3CF_3$ since the observable features for all the other allyl species described in this paper can be traced back to an analogous behavior.

In the RT ¹H NMR spectrum of $[Pd(\eta^3-C_3H_5)SNS(\mathbf{0})]SO_3CF_3$ in CDCl₃ a doublet ($\delta = 4.20$ ppm) and a quintet ($\delta = 5.98$ ppm) ascribable to the allyl terminus and the central proton, respectively, are detectable (AX₄ system). The signals attributable to the SNS ligand shift downfield upon coordination, so that thiomethyl protons CH₂-S resonate as a singlet at $\delta = 4.62$ ppm, the pyridine protons H^{3,5} are detectable as a multiplet together with the phenyl protons at $\delta = 7.30$, and the pyridine H⁴ resonates at $\delta = 7.66$ ppm as a triplet.

This behavior, which is not unprecedented,^{11f,h} was interpreted on the basis of a windshield-wiper movement of the dendritic arms which alternatively coordinate, inducing a sulfur absolute configuration inversion together with η^3 - η^1 - η^3 allyl isomerization.^{11f,h} This rearrangement, at variance with other observed fluxional phenomena,¹⁸ is concentration independent and can be interpreted on the basis of the intramolecular mechanistic path represented in Scheme 3 (intermediate **IIa**).

Analogously the RT ¹H NMR spectrum of $[Pd(\eta^3-1,1-(CH_3)_2C_3H_3)SNS(\mathbf{0})]SO_3CF_3$ is easily interpreted on the basis of similar behavior. Thus, the phenyl and the isochronous H^{3,5} pyridine protons resonate at $\delta = 7.31$ ppm, and the triplet ascribable to pyridine H⁴ and the thiomethyl CH₂-S protons are detected at $\delta = 7.63$ and 4.58 ppm, respectively. The allyl protons display an AX₂ system where the H² proton is detected as a triplet at

(16) Harley, F. R.; Jones, S. R. *J. Organomet. Chem.* **1974**, *66*, 472.

(17) Auburn, P. R.; Mackenzie, P. B.; Bosnich, B. *J. Am. Chem. Soc.* **1985**, *107*, 2033.

(18) Canovese, L.; Lucchini, V.; Santo, C.; Visentin, F.; Zambon, A. *J. Organomet. Chem.* **2002**, *642*, 58.

5.67 ppm and the $\text{CH}_2-\text{CH}-\text{C}(\text{CH}_3)_2$ as a doublet at 4.18 ppm. The methyl protons of the allyl fragment $\text{CH}_2-\text{CH}-\text{C}(\text{CH}_3)_2$ resonate as distinct singlets at $\delta = 1.51$ (anti) and 1.82 (syn) ppm.

This behavior also can be interpreted on the basis of Scheme 3. The two possible η^1 -allyl species are not isoergodic, and only on increasing the temperature does the more crowded species become accessible as an intermediate in the fluxional process, as is apparent in the spectrum at $T = 323$ K, in which the two CH_3 -singlets collapse, indicating that the $\eta^3-\eta^1-\eta^3$ isomerism via the sterically hindered **Ib** intermediate becomes operative.

The observed phenomena could not be considered unusual in the case of SNS derivatives which, with respect to their coordinating capability and steric demand, are very close to those of analogous potentially terdentate S–N–S ligands.^{11h,f} However, on increasing the size of the dendritic branch, no hints of unusual behavior can be observed since the spectral features of all the studied species are very similar independently of the concentration of the complexes, the steric demand, and electronic characteristics of the macrocones. As a matter of fact the ^1H NMR spectra of $[\text{Pd}(\eta^3-\text{C}_3\text{H}_5)\text{SNS}(\mathbf{3})]\text{SO}_3\text{CF}_3$ and $[\text{Pd}(\eta^3-1,1-(\text{CH}_3)_2\text{C}_3\text{H}_3)\text{SNS}(\mathbf{3})]\text{SO}_3\text{CF}_3$ are superimposable to those of the corresponding SNS derivatives, apart from the relative signal intensity of the protons of the coordinating site and of the allyl protons (which are almost annihilated within the skeleton signals). Apparently some sort of fluxional rearrangement is still operative without relationship to the size of the ligands.

Synthesis of Palladium(0) Fumaronitrile Complexes. The palladium(0) fumaronitrile complexes were obtained by addition of the specific dendritic ligand S–N–S to a solution containing a stoichiometric amount of $\text{Pd}_2(\text{DBA})_3\text{CHCl}_3$ ¹⁹ in the presence of a slight excess of fumaronitrile in acetone at RT under inert atmosphere (N_2).

The complexes $[\text{Pd}(\eta^2-\text{fn})\text{SNS}(\mathbf{0})]$, $[\text{Pd}(\eta^2-\text{fn})\text{SNS}(\mathbf{1})]$, $[\text{Pd}(\eta^2-\text{fn})\text{SNS}(\mathbf{2})]$, and $[\text{Pd}(\eta^2-\text{fn})\text{SNS}(\mathbf{3})]$ were obtained in 44%, 84%, 71%, and 90% yield, respectively. The ^1H NMR spectra provide an easy identification of the samples, which were however fully characterized by elemental analysis, ^{13}C NMR, and MALDI-TOF technique. In particular MALDI-TOF mass spectra show the presence of ions corresponding to $[\text{SNS Pd}]^+$ ionic species for all Pd(0) dendritic compounds. Ions at lower m/z values are also detected due to the dendritic fragmentation already observed under MALDI conditions for pyridine-based dendrimers.²⁰

Solution Behavior of Palladium(0) Fumaronitrile Complexes. Also in the case of the palladium(0) substrates it is convenient to discuss the spectral features of the SNS(0) derivative because of the more favorable signal ratio and the similarity of behavior. The most significant ^1H NMR data for the Pd(0) fumaronitrile complexes are those ascribable to olefinic protons, to $\text{CH}_2\text{-S}$ thiomethyl protons, and the signals in the aromatic region. Thus the complex $[\text{Pd}(\eta^2-\text{fn})\text{SNS}(\mathbf{0})]$ is

characterized by a singlet at $\delta = 3.21$ ppm (olefinic protons), a broad AB system at $\delta = 4.54$ ppm ($\text{CH}_2\text{-S}$), a multiplet at $\delta = 7.33$ ppm ($\text{H}^{3,5}_{\text{pyr}}$ and phenyl protons), and a triplet at $\delta = 7.61$ ppm (H^4_{pyr}). The solution behavior of palladium(0) species is interpreted on the basis of a fluxional rearrangement which takes into account the apparent symmetry of the substrate described by the above-mentioned spectrum. This feature is in fact inconsistent with a structure bearing a terdentate ligand which can only act as a bidentate arm-off species in a square planar environment shared with an η^2 -coordinated olefin. Again the “windshield-wiper” motion of the two branches induces a generalized symmetry that can be traced back to the formation of an intermediate species with two peripheral partially bound sulfur atoms. The fumaronitrile remains tightly η^2 -coordinated, as can be deduced from the residual AB system at $\delta = 4.54$ ppm ($\text{CH}_2\text{-S}$) determined by the presence of chiral palladium, which does not change its absolute configuration as dictated by the olefin face coordinated to the metal. Obviously, under these circumstances the AB system could not stem from the chirality of the sulfur, which rapidly inverts its absolute configuration through the fast “windshield-wiper” motion. Again, no particular differences among the ^1H NMR spectra describing the fluxional rearrangement of the complexes bearing different dendritic wedges can be observed; the detected behaviors seem independent of the size of ancillary ligands also with the palladium(0) substrates.

Allyl Amination Reactions. The allyl amination reactions were monitored both by ^1H NMR spectrometry and by UV–vis spectroscopy (vide infra). Formation of the corresponding $[\text{Pd}(\eta^2-\text{fn})(\text{S}-\text{N}-\text{S})]$ species and the piperidine-allyl derivatives was confirmed by comparison of the ensuing ^1H NMR spectra with those of authentic samples independently synthesized.

Kinetics and Mechanism of the Allyl Amination Reaction. The complexes $[\text{Pd}(\eta^3\text{-allyl})(\text{SNS})]$ react at 25 °C in CHCl_3 with piperidine in the presence of fumaronitrile (fn) to give the corresponding palladium(0) fumaronitrile complexes and allylpiperidine.

All the reactions were followed by monitoring UV–vis absorbance changes in the wavelength range 500–280 nm (or at selected wavelengths) of CHCl_3 solutions of the allyl complexes **A** ($[\text{Pd}]_0 \cong 1 \times 10^{-4}$ mol dm^{-3}) in the presence of fn ($(2-8) \times 10^{-4}$ mol dm^{-3}) and an excess of terdentate S–N–S ligand ($\geq 1 \times 10^{-3}$ mol dm^{-3}). Under these conditions the reactions went smoothly to completion, as can be seen by comparison of the final spectra obtained after seven (or eight) half-lives with those of the authentic final products independently synthesized. The conversion of **A** into **B** with time appeared to obey the monoexponential relationship $A_t = A_\infty + (A_0 - A_\infty) \exp(-k_{\text{obs}}t)$, corresponding to a pseudo-first-order process:

$$-d[\mathbf{A}]/dt = k_{\text{obs}}[\mathbf{A}] \quad (1)$$

The k_{obs} values, calculated by nonlinear regression analysis of A_t (absorbance at time t) versus t (time), show a bivariate dependence on entering piperidine HY and added SNS ligand concentration (both considered as constant, being in large excess over the metal), whereas the fumaronitrile concentration does not affect

(19) Ukai, T.; Kawazura, H.; Ishii, Y.; Bonnet, J. J.; Ibers, J. A. *J. Organomet. Chem.* **1974**, *65*, 253.

(20) Chessa, G.; Scrivanti, A.; Seraglia, R.; Traldi, P. *Rapid Commun. Mass Spectrom.* **1998**, *12*, 1533.

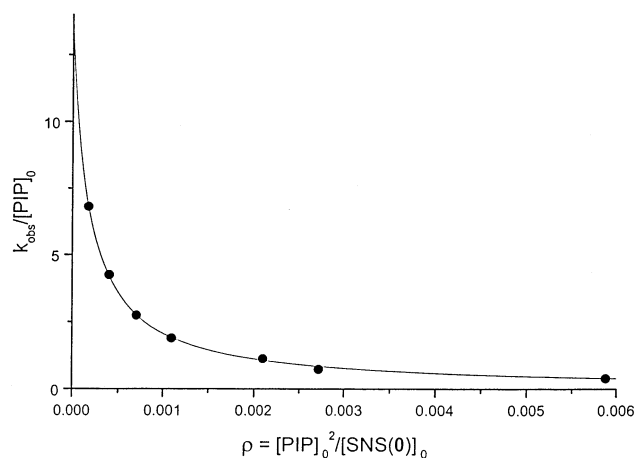


Figure 1. Dependence of $k_{\text{obs}}/[\text{PIP}]_0$ on $[\text{PIP}]_0^2/[\text{SNS}(\mathbf{0})]_0$ for reaction of $[\text{Pd}(\eta^3\text{-allyl})\text{SNS}(\mathbf{0})]$ with piperidine in CHCl_3 at 25 °C.

Table 1. Second-Order Rate Constants (k_2) and Equilibrium Constants (K_E) for Reactions of Palladium Allyl Complexes with Piperidine at 25 °C in CHCl_3

| complex | k_2 ($\text{mol}^{-1}\cdot\text{dm}^3\cdot\text{s}^{-1}$) | K_E |
|--|---|-------------------|
| $[\text{Pd}(\eta^3\text{-C}_3\text{H}_5)\text{SNS}(\mathbf{0})]^+$ | 13.6 ± 0.4 | 5335 ± 263 |
| $[\text{Pd}(\eta^3\text{-C}_3\text{H}_5)\text{SNS}(\mathbf{1})]^+$ | 13.9 ± 0.3 | 8677 ± 403 |
| $[\text{Pd}(\eta^3\text{-C}_3\text{H}_5)\text{SNS}(\mathbf{2})]^+$ | 6.7 ± 0.3 | 9728 ± 945 |
| $[\text{Pd}(\eta^3\text{-C}_3\text{H}_5)\text{SNS}(\mathbf{3})]^+$ | 0.7 ± 0.4 | 42000 ± 20000 |

the observed rate constants. Such dependence can be described by eq 2:

$$k_{\text{obs}} = k_2[\text{HY}]/(1 + K_E[\text{HY}]^2/[\text{SNS}]) \quad (2)$$

which can be rewritten as

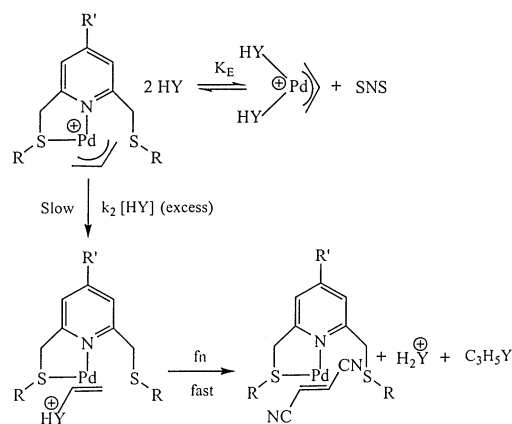
$$k_{\text{obs}}/[\text{HY}] = k_2/(1 + K_E\rho) \quad (3)$$

where $\rho = [\text{HY}]^2/[\text{SNS}]$.

The parameters k_2 and K_E were determined by nonlinear regression of rate constants to eq 3 (Figure 1), while the values of k_2 and K_E are listed in Table 1.

Such a dependence was interpreted on the basis of the stepwise mechanism of Scheme 4. This mechanism appears to be common to the whole class of reactions involving allyl amination of allyl palladium complexes with both bi- or terdentate pyridylmethanimine, pyridylthioether, or pyridylselenoether ligands,¹¹ irrespectively of their nucleophilic capabilities, electronic characteristics, and steric requirements. The role of these properties may become of paramount importance in relation to the size and complexity of the dendritic cone containing the metal-allyl species since it is possible to distinguish between the slow attack on the allyl fragment (k_2) and the fast and concomitant displacement of the palladium-coordinated ancillary ligand (K_E), thereby gathering information on the accessibility of both the reaction centers. In any case, the accessibility of the metal center seems warranted irrespectively of the dendritic size (vide infra). However, as can be seen in Table 1, the size of the dendritic cone becomes relevant only starting from the $[\text{Pd}(\eta^3\text{-C}_3\text{H}_5)\text{SNS}(\mathbf{3})]$ complex. Apparently, some sort of structural phenomenon abruptly occurs on going from the second- to the third-generation dendrimeric complex. The trend of k_2

Scheme 4



R = C_6H_5 ; DENDRITIC WEDGES

R' = H; $\text{OCH}_2\text{C}_6\text{H}_5$

HY = PIPERIDINE

can be easily explained on the basis of the increased steric hindrance of the dendritic branches influencing the rate of associative attack of piperidine on the coordinated allyl fragment. In this respect the decreasing k_2 value on going from first to third dendrimer generation is not surprising even if the k_2 value seems to be slightly affected up to the second generation, since the reactivity appears to be hardly modulated by the substantial increase in the steric demand of the branches. Rearrangement in solution would leave the allyl fragment equally prone to the piperidine attack until no rearrangement could compensate for the ensuing steric hindrance of the third-generation dendrimeric complex. The drop in reaction rate (1 order of magnitude) bears witness to this very fact.

On the other hand, the degree of displacement of the ligand by the incoming piperidine as testified by the value of the thermodynamic parameter K_E parallels the observed reaction rate trend. Again the value of the equilibrium constant suddenly increases when the third-generation complex $[\text{Pd}(\eta^3\text{-C}_3\text{H}_5)\text{SNS}(\mathbf{3})]$ is investigated. The magnitude of K_E was shown to increase with the decreasing nucleophilic capability of pyridyl nitrogen and thioetheric sulfur but also with the release of steric strain,^{11g-1} which becomes very important in the case of the sterically hindered $[\text{Pd}(\eta^3\text{-C}_3\text{H}_5)\text{SNS}(\mathbf{3})]$ complex. Apparently, the electrostatic interaction between the dendritic branches induces severe distortion of the complex coordination plane and concomitant destabilization of the whole structure. The change in reactivity as a consequence of the increasing size of the ligand molecules involved can be thus traced back to a conformational change in the substrates. Chow and co-workers demonstrated that the Diels–Alder reaction catalyzed by copper complexes bearing bis(oxazoline) dendrimers as chelating agents can be strongly reduced on going from the second to the third ligand generation⁷ and that such behavior is attributable to a folding-back of the dendritic structure, which determines an increased steric hindrance at the copper reactive site.

Thus, in the present work the observed discontinuity in the thermodynamic and kinetic parameters on going from second- to third-generation metal dendrimers may correspond to the transition from extended to globular

configuration of the dendritic branches, as dictated by their steric and electronic interaction, which would increase both the steric hindrance and distortion at the reactive metal core. Therefore, the concomitant changes in k_2 and K_E are easily understood. However, since no particular differences among different generation metal dendrimers can be gathered from analysis of the RT ^1H NMR spectra with respect to the fluxional phenomena (which would be strongly influenced by the size of the wedges), one may postulate an alternative explanation to the accepted windshield-wiper motion of the dendritic wings. Thus, we tentatively entertain the intriguing hypothesis that it is the metal itself that migrates within the potentially terdentate coordinative site, thereby inducing the observed fluxional rearrangement. Work is in progress in our laboratory in order to confirm this view and gather more information about this phenomenon.

Conclusion

A series of pyridyl-dithioether-based Pd(II) and Pd(0) metallo dendrimers were successfully synthesized and characterized by NMR, elemental analysis, and MALDI-TOF determinations. The reactivity of the Pd(II) allyl complexes was also studied with respect to the allyl amination by piperidine, and the results obtained were compared and discussed in terms of increasing wedge size. The kinetic and thermodynamic behavior of the species is hardly influenced by the dendrimer generation. Only the SNS(**3**) allyl palladium derivative shows markedly different values in both allyl amination rate and ligand displacement constant, and this finding was traced back to the configuration assumed in solution upon the electronic and steric interaction of the third-generation SNS moiety. Such a configuration would increase the steric hindrance on the allyl fragment and the distortion of the main coordination plane around the metal, thereby imparting the observed reactivity to the system.

Experimental Section

General Comments. 2,6-Bis(phenylthiomethyl)pyridine (SNS),²⁰ 4-mercaptobenzyl alcohol,¹⁵ 4-benzyloxy-2,6-bis(chloromethyl)pyridine,^{13,14} diethyl 4-hydroxypyridine-2,6-dicarboxylate, and second- and third-generation dendritic fragments (EtO₂C)₄-[Py]₃-OH and (EtO₂C)₈-[Py]₇-OH were prepared according to literature procedures.¹³

Tetrahydrofuran (THF) was distilled from Na-benzophenone immediately before use. Dimethyl sulfoxide (DMSO) and acetone were dried and stored over 3 Å and 4 Å molecular sieves, respectively. *N,N*-Dimethylformamide (DMF) was purified by distillation from CaH₂ and stored over 4 Å molecular sieves in a dark bottle. Dichloromethane was freshly distilled from CaH₂. Other solvents and reagents were generally used without further purification. Column chromatography was performed using silica gel (SiO₂, Macherey Nagel, 0.04–0.063 mm, 230–400 mesh).

^1H and ^{13}C NMR spectra were obtained on a Bruker AC 200 or on a Bruker Avance 300 spectrometer using the solvent signal as internal standard. The infrared spectra were recorded on a Nicolet Magna-IR 750 spectrometer as KBr pellets. Melting points were taken in capillary tubes with a Buchi 535 apparatus and are uncorrected.

Mass spectra of dendrimers were obtained by matrix-assisted laser desorption ionization mass spectrometry (MALDI-

MS) using a reflex time-of-flight instrument (Bruker-Franzen Analytik) equipped with a "Scout" ion source operating in positive linear mode (instrumental conditions: nitrogen laser $\lambda = 337$ nm; laser energy = 50 μJ ; acceleration voltage = 25 kV). Dithranol was used as matrix laid down in solution with the sample (solvent: chloroform).

Synthesis of Ligands. 4-Benzyloxy-2,6-bis(4-hydroxymethylphenylthiomethyl)pyridine, 2. A suspension of K₂CO₃ (995 mg, 7.2 mmol) and thiol (845 mg, 6.03 mmol) in dry DMF (30 mL) was stirred at room temperature under reduced pressure for 30 min, after which 4-benzyloxy-2,6-bis(chloromethyl)pyridine (810 mg, 2.87 mmol) and 18-crown-6 (152 mg, 0.574 mmol) were added, and the reaction mixture was heated at 45 °C for 24 h under an atmosphere of argon. After evaporation of the solvent the organic product was extracted with CH₂Cl₂ (150 mL). The organic extract was washed with brine (2 × 75 mL), dried (Na₂SO₄), and evaporated under reduced pressure. The crude product was purified by flash chromatography eluting with 10% EtOAc in CH₂Cl₂, gradually increasing to 60%, to give **2** as a white solid (1.18 g, 84%). Mp: 106–107 °C. ^1H NMR (CDCl₃): δ 2.42 (bs, 2H, OH), 4.20 (s, 4H, CH₂S), 4.61 (s, 4H, CH₂OH), 5.00 (s, 2H, PhCH₂O), 6.87 (s, 2H, pyr-H_{3,5}), 7.23 (m, 8H, Ph-H), 7.37 (5H, m Ph-H). ^{13}C NMR (CDCl₃): δ 39.8 (CH₂S), 64.5 (CH₂OH), 69.9 (CH₂O), 108.2 (pyr-C_{3,5}), 127.4, 127.5, 128.3, 128.6, 129.3, 134.7, 135.4, and 139.1 (Ph-C), 158.8 (pyr-C_{2,6}), 166.2 (pyr-C₄). IR (cm⁻¹): 3290 (br, OH). Anal. Calcd for C₂₈H₂₇NO₃S₂: C, 68.69; H, 5.56; N, 2.86. Found: C, 68.59; H, 5.34; N, 2.86.

4-Benzyloxy-2,6-bis(4-chloromethylphenylthiomethyl)pyridine, 3. A solution of dialcohol **2** (1.156 g, 2.38 mmol) in SOCl₂ (15 mL) was heated at 50 °C for 4 h, after which the excess of SOCl₂ was evaporated and the residue was neutralized with 10% aqueous Na₂CO₃. The aqueous phase was extracted with CH₂Cl₂ (150 mL). The organic extract was washed with water, dried (Na₂SO₄), and evaporated under reduced pressure. Purification by flash chromatography eluting sequentially with CH₂Cl₂ and 2% Et₂O in CH₂Cl₂ gave the chloride **3** (1.025 g, 82%). Mp: 133–133.5 °C. ^1H NMR (CDCl₃): δ 4.23 (s, 4H, CH₂S), 4.54 (s, 4H, CH₂Cl), 4.99 (s, 2H, PhCH₂O), 6.84 (s, 2H, pyr-H_{3,5}), 7.28 (m, 8H, Ph-H), 7.36 (m, 5H, Ph-H). ^{13}C NMR (CDCl₃): δ 39.7 (CH₂S), 45.8 (CH₂-Cl), 69.9 (CH₂O), 108.2 (pyr-C_{3,5}), 127.6, 128.4, 128.7, 129.1, 129.2, 135.3, 135.4, and 136.5 (Ph-C), 158.6 (pyr-C_{2,6}), 166.2 (pyr-C₄). IR (cm⁻¹): 1263 (CH₂Cl). Anal. Calcd for C₂₈H₂₅Cl₂NO₃S₂: C, 63.87; H, 4.79; N, 2.66. Found: C, 63.71; H, 4.62; N, 2.59.

SNS(1), 7. A mixture of diethyl 4-hydroxypyridine-2,6-dicarboxylate, **4** (421 mg, 1.76 mmol), and anhydrous K₂CO₃ (243 mg, 1.76 mmol) in dry DMF (10 mL) was stirred at 25 °C under reduced pressure for 30 min, then 4-benzyloxy-2,6-bis(4-chloromethylphenylthiomethyl)pyridine, **3** (421 mg, 0.8 mmol), was added and the reaction mixture was allowed to react at 70 °C for 24 h under a nitrogen atmosphere. After removal of the solvent from the reaction mixture the resulting residue was extracted with CH₂Cl₂ (100 mL). The organic extract was washed with brine, dried (Na₂SO₄), and finally evaporated. The crude product was purified by flash chromatography eluting with 2% MeOH in CH₂Cl₂ to give **7** as a glassy solid (690 mg, 92%). ^1H NMR (CDCl₃): δ 1.46 (t, 12H, $J = 7.1$ Hz, CH₂CH₃), 4.23 (s, 4H, CH₂S), 4.47 (q, 8H, $J = 7.1$ Hz, CH₂-CH₃), 5.01 (s, 2H, PhCH₂O), 5.15 (s, 4H, CH₂Opyr), 6.87 (s, 2H, pyr-H_{3,5}), 7.35 (m, 13H, Ph-H), 7.84 (s, 4H, pyr-H_{3,5}). ^{13}C NMR (CDCl₃): δ 13.9 (CH₃CH₂), 39.7 (CH₂S), 62.1 (CH₃CH₂), 69.6 and 70.0 (CH₂O), 107.9 and 114.2 (pyr-C_{3,5}), 127.3, 128.0, 128.1, 128.4, 128.9, 132.2, 135.2, and 136.9 (Ph-C), 150.0 and 158.4 (pyr-C_{2,6}), 164.4 (C=O), 165.8 and 166.2 (pyr-C₄). IR (cm⁻¹): 1744 and 1719 (C=O). MALDI-MS: m/z 955 ([M + Na]⁺). Anal. Calcd for C₅₀H₄₉N₃O₁₁S₂: C, 64.43; H, 5.30; N, 4.51. Found: C, 63.64; H, 5.19; N, 4.46.

SNS(2), 8. Compound **8** was prepared by the same synthetic procedure as described for **7** starting from the dendritic

tetraester HO-[Py]₃-(CO₂Et)₄ **5** (944 mg, 1.58 mmol), anhydrous K₂CO₃ (260 mg, 1.88 mmol), and 4-benzyloxy-2,6-bis(4-chloromethylphenylthiomethyl)pyridine, **3** (395 mg, 0.75 mmol), in dry DMF (20 mL). Purification by flash chromatography eluting with 3% MeOH in CH₂Cl₂ gave **8** as a glassy solid (1.05 g, 85%). ¹H NMR (CDCl₃): δ 1.45 (t, 24H, *J* = 7.1 Hz, CH₂CH₃), 4.23 (s, 4H, CH₂S), 4.47 (q, 16H, *J* = 7.1 Hz, CH₂CH₃), 5.00 (s, 2H, PhCH₂O), 5.07 (s, 4H, CH₂Opyr), 5.29 (s, 8H, pyrCH₂Opyr), 6.88 (s, 2H, pyr-H_{3,5}), 7.03 (s, 4H, pyr-H_{3,5}), 7.32 (m 13 H, Ph-H), 7.89 (s, 8H, pyr-H_{3,5}). ¹³C NMR (CDCl₃): δ 13.9 (CH₃-CH₂), 39.6 (CH₂S), 62.2 (CH₃CH₂), 69.6 and 70.5 (CH₂O), 107.4, 107.9, and 114.3 (pyr-C_{3,5}), 127.3, 128.0, 128.1, 128.4, 128.8, 132.6, 135.2, and 136.7 (Ph-C), 150.1, 156.4, and 158.4 (pyr-C_{2,6}), 164.2 (C=O), 165.8, 165.9, and 166.3 (pyr-C₄). IR (cm⁻¹): 1745 and 1720 (C=O). MALDI-MS: *m/z* 1673 ([M + Na]⁺). Anal. Calcd for C₈₆H₈₅N₇O₂₃S₂: C, 62.65; H, 5.20; N, 5.95. Found: C, 61.31; H, 4.99; N, 5.79.

SNS(3), **9**. Compound **9** was prepared as described for **7** starting from the dendron (CO₂Et)₈-[Py]₇-OH **6** (1.2 g, 0.91 mmol), anhydrous K₂CO₃ (0.133 g, 0.96 mmol), 18-crown-6 (24 mg, 0.09 mmol), and 4-benzyloxy-2,6-bis(4-chloromethylphenylthiomethyl)pyridine, **3** (0.226 g, 0.43 mmol), in dry DMF (20 mL) at 50 °C for 48 h. The crude product was purified by flash chromatography eluting with 3% MeOH in CH₂Cl₂ and finally recrystallized from CH₂Cl₂/EtOH (1:2, 15 mL) to give **9** as an amorphous white solid (1.101 g, 82%). ¹H NMR (CDCl₃): δ 1.44 (t, 48H, *J* = 7.1 Hz, CH₂CH₃), 4.21 (s, 4H, CH₂S), 4.46 (q, 32H, *J* = 7.1 Hz, CH₂CH₃), 4.99 (s, 2H, PhCH₂O), 5.06 (s, 4H, CH₂Opyr), 5.21 (s, 8H, pyrCH₂Opyr), 5.32 (s, 16H, pyrCH₂Opyr), 6.86 (s, 2H, pyr-H_{3,5}), 7.00 (s, 4H, pyr-H_{3,5}), 7.09 (s, 8H, pyr-H_{3,5}), 7.31 (m 13 H, Ph-H), and 7.90 (s, 16H, pyr-H_{3,5}). ¹³C NMR (CDCl₃): δ 13.9 (CH₃CH₂), 39.7 (CH₂S), 62.2 (CH₃CH₂), 69.6, 70.2, and 70.5 (CH₂O), 107.2, 107.3, 107.9, and 114.3 (pyr-C_{3,5}), 127.3, 128.0, 128.4, 128.6, 132.6, 135.2, and 136.8 (Ph-C), 150.1, 156.7, 156.8, and 158.3 (pyr-C_{2,6}), 164.2 (C=O), 165.8, 165.9, 166.0, and 166.3 (pyr-C₄). IR (cm⁻¹): 1745 and 1720 (C=O). MALDI-MS: *m/z* 3106 ([M + Na]⁺). Anal. Calcd for C₁₅₈H₁₅₇N₁₅O₄₇S₂·H₂O·CHCl₃: C, 59.32; H, 5.01; N, 6.53. Found: C, 60.57; H, 4.76; N, 6.55.

Synthesis of Palladium(II) Complexes. [Pd(η³-C₃H₅)SNS(0)]SO₃CF₃. To a solution of 87.1 mg (0.238 mmol) of [Pd₂(μ-Cl)₂(η³-C₃H₅)₂] in freshly distilled CH₂Cl₂ (10 mL) was added 123.3 mg (0.479 mmol) of AgSO₃CF₃ under inert atmosphere (N₂). The solution, magnetically stirred, was reacted in the dark for 4 h. To the filtered solution was added 161.8 mg (0.5 mmol) of 2,6-bis(phenylthiomethyl)pyridine (SNS) ligand. The resulting mixture was stirred for 30 min and finally treated with activated charcoal for 10 min and filtered on Celite filter. Addition of Et₂O to the cooled (ice bath) and concentrated solution yields 235.6 mg (0.38 mmol 76%) of the title complex as a whitish precipitate. ¹H NMR (CDCl₃): δ 4.20 (d, 4H, *J* = 9.8 Hz, all-CH₂), 4.62 (s, 4H, CH₂S), 5.98 (q, 1H, *J* = 9.8 Hz, all-CH), 7.19–7.43 (m, 12H, pyr-H_{3,5} and Ph-H), 7.66 (t, 1H, *J* = 7.8 Hz, pyr-H₄). ¹³C NMR (CDCl₃): δ 47.1 (CH₂S), 67.4 (all-CH₂), 118.8 (all-CH), 124.5 (pyr-C_{3,5}), 129.6, 130.1, 131.3, and 132.2 (Ph-C), 140.4 (pyr-C₄), 159.4 (pyr-C_{2,6}). Anal. Calcd for C₂₃H₂₃F₃NO₃PdS₃: C, 44.48; H, 3.73; N, 2.26. Found: C, 44.32; H, 3.98; N, 2.51.

[Pd(η³-C₃H₅)SNS(1)]SO₃CF₃. The title compound was obtained as the [Pd(η³-C₃H₅)(SNS)]SO₃CF₃ complex using SNS-(1) as ligand. Yield: 75% (whitish powder). ¹H NMR (CDCl₃): δ 1.45 (t, 12H, *J* = 7.1 Hz, CH₂CH₃), 3.99 (bs, 4H, all-CH₂), 4.45 (q, 8H, *J* = 7.1 Hz, CH₂CH₃), 4.56 (s, 4H, CH₂S), 5.08 (s, 2H, PhCH₂O), 5.18 (s, 4H, CH₂Opyr), 5.79 (bq, 1H, all-CH, *J* = 9.9 Hz), 6.97 (s, 2H, pyr-H_{3,5}), 7.32–7.51 (m, 13H, Ph-H), 7.82 (s, 4H, pyr-H_{3,5}). ¹³C NMR (CDCl₃): δ 14.6 (CH₃CH₂), 45.3 (CH₂S), 62.9 (CH₃CH₂), 66.3 (all-CH₂), 70.3 and 71.4 (CH₂O), 110.9 and 114.9 (pyr-C_{3,5}), 117.2 (all-CH), 128.1, 129.1, 129.2, 131.7, 133.3, 135.0, and 135.7 (Ph-C), 150.7 and 160.0 (pyr-C_{2,6}), 165.0 (C=O), 166.7 and 167.4 (pyr-C₄). IR (cm⁻¹): 1744 and 1720 (C=O). MALDI-MS: *m/z* 1042 ([SNS(1)Pd]⁺), 1082

([SNS(1)PdC₃H₆]⁺). Anal. Calcd for C₅₄H₅₅F₃N₃O₁₄PdS₃C: C, 52.75; H, 4.51; N, 3.42. Found: C, 52.70; H, 4.68; N, 3.26.

[Pd(η³-C₃H₅)SNS(2)]SO₃CF₃. The title compound was obtained as the [Pd(η³-C₃H₅)(SNS)]SO₃CF₃ complex using SNS-(2) as ligand. Yield: 59% (whitish powder). ¹H NMR (CDCl₃): δ 1.45 (t, 12H, CH₂CH₃, *J* = 7.1 Hz), 3.97 (bs, 4H, all-CH₂), 4.45 (q, 8H, *J* = 7.1 Hz, CH₂CH₃), 4.49 (s, 4H, CH₂S), 5.07 (s, 2H, PhCH₂O), 5.10 (s, 4H, CH₂Opyr), 5.30 (s, 8H, pyrCH₂Opyr), 5.74 (bq, 1H, all-CH), 7.02 (bs, 6H, pyr-H_{3,5}), 7.24–7.47 (m, 13H, Ph-H), 7.89 (s, 8H, pyr-H_{3,5}). ¹³C NMR (CDCl₃): δ 14.6 (CH₃CH₂), 44.9 (CH₂S), 62.9 (CH₃CH₂), 66.1 (all-CH₂), 69.9 and 71.2 (CH₂O), 108.0, 110.6, and 115.0 (pyr-C_{3,5}), 116.8 (all-CH), 128.1, 128.9, 129.0, 129.2, 130.9, 135.1, and 135.5 (Ph-C), 150.8, 157.3, and 159.8 (pyr-C_{2,6}), 164.9 (C=O), 166.6, 166.9, and 167.3 (pyr-C₄). MALDI-MS: *m/z* 1758 ([SNS(2)Pd]⁺), 1799 ([SNS(2)PdC₃H₆]⁺). IR (cm⁻¹): 1742 and 1724 (C=O). Anal. Calcd for C₉₀H₉₁F₃N₇O₂₆PdS₃: C, 55.54; H, 4.71; N, 5.04. Found: C, 55.66; H, 4.58; N, 4.79.

[Pd(η³-C₃H₅)SNS(3)]SO₃CF₃. The title compound was obtained as the [Pd(η³-C₃H₅)(SNS)]SO₃CF₃ complex using SNS-(3) as ligand. Yield: 86% (whitish powder). ¹H NMR (CDCl₃): δ 1.43 (t, 48H, *J* = 7.1 Hz, CH₂CH₃), 4.09 (bd, 2H, all-CH₂), 4.43 (q, 32H, *J* = 7.1 Hz, CH₂CH₃), 4.59 (bs, 4H, CH₂S), 5.09 (bs, 6H, CH₂Opyr and PhCH₂O), 5.20 (s, 8H, pyrCH₂Opyr), 5.31 (s, 16H, pyrCH₂Opyr), 7.01 (s, 6H, pyr-H_{3,5}), 7.09 (s, 8H, pyr-H_{3,5}), 7.31–7.52 (m 13 H, Ph-H), and 7.89 (s, 16H, pyr-H_{3,5}). ¹³C NMR (CDCl₃): δ 13.9 (CH₃CH₂), 46.0 (CH₂S), 62.2 (CH₃CH₂), 66.9 (all-CH₂), 69.0, 70.2, 70.5, and 70.9 (CH₂O), 107.1, 107.4, 110.6, and 114.3 (pyr-C_{3,5}), 117.5 (all-CH), 127.5, 128.0, 128.5, 128.6, 131.0, 131.4, 134.0, and 136.1 (Ph-C), 150.1, 156.6, 156.9, and 159.4 (pyr-C_{2,6}), 164.2 (C=O), 165.9, 166.0, and 167.0 (pyr-C₄). IR (cm⁻¹): 1743 and 1721 (C=O). MALDI-MS: *m/z* 3190 ([SNS(3)Pd]⁺), 3231 ([SNS(3)PdC₃H₆]⁺). Anal. Calcd for C₁₆₂H₁₆₃F₃N₁₅O₅₀PdS₃: C, 57.57; H, 4.86; N, 6.22. Found: C, 57.44; H, 4.80; N, 6.21.

[Pd(η³-1,1-(CH₃)₂C₃H₃)SNS(0)]SO₃CF₃. The title compound was obtained following the usual synthetic scheme using [Pd₂(μ-Cl)₂(η³-1,1-(CH₃)₂C₃H₃)₂] as starting material and SNS(0) as ligand. Yield: 73% (whitish powder). ¹H NMR (CDCl₃): δ 1.51 (s, 3H, all-CH₃ anti), 1.82 (s, 3H, all-CH₃ syn), 4.18 (d, 2H, *J* = 10.4 Hz, all-CH₂), 5.58 (s, 4H, CH₂S), 5.67 (t, 1H, *J* = 10.4 Hz, all-CH), 7.16–7.45 (m, 2H, pyr-H_{3,5} and Ph-H), 7.63 (t, 1H, *J* = 7.7 Hz, pyr-H₄). ¹³C NMR (CDCl₃): δ 23.3 (all-CH₃ anti), 29.3 (all-CH₃ syn), 46.8 (CH₂S), 62.5 (all-CH₂), 99.3 (all-C(CH₃)₂), 112.4 (all-CH), 124.7 (pyr-C_{3,5}), 129.7, 130.2, 131.1, and 132.2 (Ph-C), 140.3 (pyr-C₄), 159.5 (pyr-C_{2,6}). Anal. Calcd for C₂₅H₂₇F₃NO₃PdS₃: C, 46.26; H, 4.19; N, 2.16. Found: C, 46.06; H, 4.02; N, 2.11.

[Pd(η³-1,1-(CH₃)₂C₃H₃)SNS(1)]SO₃CF₃. The title compound was obtained as the [Pd(η³-1,1-(CH₃)₂C₃H₃)SNS(0)]SO₃CF₃ complex using SNS(1) as ligand. Yield: 73% (whitish powder). ¹H NMR (CDCl₃): δ 1.44 (t, 12H, *J* = 7.1 Hz, CH₂CH₃), 1.48 (bs, 3H, all-CH₃ anti), 1.80 (s, 3H, all-CH₃ syn), 4.11 (d, 2H, *J* = 10.5 Hz, all-CH₂), 4.45 (q, 8H, *J* = 7.1 Hz, CH₂CH₃), 4.52 (s, 4H, CH₂S), 5.10 (s, 2H, PhCH₂O), 5.20 (s, 4H, CH₂Opyr), 5.56 (t, 1H, all-CH, *J* = 10.5 Hz), 6.97 (s, 2H, pyr-H_{3,5}), 7.31–7.58 (m, 13H, Ph-H), 7.83 (s, 4H, pyr-H_{3,5}). ¹³C NMR (CDCl₃): δ 14.6 (CH₃CH₂), 23.2 (all-CH₃ anti), 29.3 (all-CH₃ syn), 46.7 (CH₂S), 62.5 (all-CH₂), 62.9 (CH₃CH₂), 70.1 and 71.6 (CH₂O), 99.8 (all-C(CH₃)₂), 111.9 (all-CH), 111.5 and 114.9 (pyr-C_{3,5}), 128.2, 129.0, 129.1, 129.2, 132.0, 132.4, 134.9, and 136.6 (Ph-C), 150.8 and 160.6 (pyr-C_{2,6}), 165.0 (C=O), 166.7 and 167.5 (pyr-C₄). IR (cm⁻¹): 1744 and 1720 (C=O). MALDI-MS: *m/z* 1041 ([SNS(1)Pd]⁺), 1110 ([SNS(1)PdC₅H₁₀]⁺). Anal. Calcd for C₅₆H₅₈F₃N₃O₁₄PdS₃: C, 53.52; H, 4.65; N, 3.34. Found: C, 53.45; H, 4.71; N, 3.36.

[Pd(η³-1,1-(CH₃)₂C₃H₃)SNS(2)]SO₃CF₃. The title compound was obtained as the [Pd(η³-1,1-(CH₃)₂C₃H₃)SNS(0)]SO₃CF₃ complex using SNS(2) as ligand. Yield: 73% (whitish powder). ¹H NMR (CDCl₃): δ 1.36 (s, 3H, all-CH₃ anti), 1.44 (t, 24H, *J* = 7.1 Hz, CH₂CH₃), 1.66 (s, 3H, all-CH₃ syn), 3.86 (bs,

2H, all-CH₂), 4.45 (q, 16H, $J = 7.1$ Hz CH₂CH₃), 4.47 (bs, 4H, CH₂S), 5.05 (s, 2H, PhCH₂O), 5.09 (s, 4H, CH₂Opyr), 5.29 (s, 8H, pyrCH₂Opyr), 5.64 (bt, 1H, all-CH), 6.97 (s, 2H, pyr-H_{3,5}), 7.03 (s, 4H, pyr-H_{3,5}), 7.28–7.49 (m, 13H, Ph-H), 7.89 (s, 8H, pyr-H_{3,5}). ¹³C NMR (CDCl₃): δ 14.6 (CH₃CH₂), 22.7 (all-CH₃ anti), 28.4 (all-CH₃ syn), 44.9 (CH₂S), 62.9 (CH₃CH₂ and all-CH₂), 70.0 and 71.2 (CH₂O), 97.7 (all-C(CH₃)₂), 110.4 (all-CH and pyr-C_{3,5}), 108.0, and 115.0 (pyr-C_{3,5}), 128.1, 128.9, 129.1, 130.6, 135.3, and 135.5 (Ph-C), 150.8, 157.2, and 159.7 (pyr-C_{2,6}), 164.9 (C=O), 166.6, 166.9, and 167.0 (pyr-C₄). IR (cm⁻¹): 1743 and 1724 (C=O). MALDI-MS: m/z 1758 ([SNS(2)Pd]⁺), 1826 ([SNS(2)PdC₅H₁₀]⁺). Anal. Calcd for C₉₂H₉₄F₃N₇O₂₆PdS₃: C, 55.99; H, 4.80; N, 4.97. Found: C, 55.85; H, 4.63; N, 4.72.

[Pd(η^3 -1,1-(CH₃)₂C₃H₃)SNS(3)]SO₃CF₃. The title compound was obtained as the [Pd(η^3 -1,1-(CH₃)₂C₃H₃)SNS(0)]SO₃CF₃ complex using SNS(3) as ligand. Yield: 88% (whitish powder). ¹H NMR (CDCl₃): δ 1.43 (t, 51H, $J = 7.1$ Hz, CH₂CH₃ and all-CH₃ anti), 1.69 (s, 3H, all-CH₃ syn), 4.06 (bd, 2H, all-CH₂), 4.45 (q, 32H, $J = 7.1$ Hz, CH₂CH₃), 4.54 (bs, 4H, CH₂S), 5.10 (bs, 6H, CH₂Opyr and PhCH₂O), 5.20 (s, 8H, pyrCH₂Opyr) 5.30 (s, 16H, pyrCH₂Opyr), 5.50 (bt, 1H, all-CH), 7.01 (s, 6H, pyr-H_{3,5}), 7.09 (s, 8H, pyr-H_{3,5}), 7.30–7.50 (m, 13H, Ph-H), and 7.88 (s, 16H, pyr-H_{3,5}). ¹³C NMR (CDCl₃): δ 14.6 (CH₃CH₂), 22.9 (all-CH₃ anti), 29.0 (all-CH₃ syn), 46.7 (CH₂S), 62.9 (all-CH₂), 62.8 (CH₃CH₂), 69.7, 70.9, 71.2, and 71.6 (CH₂O), 99.1 (all-C(CH₃)₂), 107.8, 108.1, 111.5, and 114.9 (pyr-C_{3,5}), 112.2 (all-CH), 128.2, 128.7, 129.1, 129.5, 131.8, 132.5, 134.8, and 137.0 (Ph-C), 150.8, 157.3, 157.6, and 160.4 (pyr-C_{2,6}), 164.9 (C=O), 166.6, 166.7, and 167.6 (pyr-C₄). IR (cm⁻¹): 1744 and 1720 (C=O). MALDI-MS: m/z 3189 ([SNS(3)Pd]⁺), 3257 ([SNS(3)PdC₅H₁₀]⁺). Anal. Calcd for C₁₆₄H₁₆₆F₃N₁₅O₅₀PdS₃: C, 57.82; H, 4.91; N, 6.17. Found: C, 57.57; H, 4.71; N, 6.08.

Synthesis of Palladium(0) Complexes. [Pd(η^2 -fn)SNS(0)]. A 23.8 mg (0.305 mmol) sample of fumaronitrile and 94.4 mg (0.292 mmol) of 2,6-diphenylthiomethylpyridine (SNS(0)) were dissolved in 15 mL of freshly distilled acetone under inert atmosphere (N₂). A 150 mg (0.145 mmol) sample of Pd₂DBA₃·CHCl₃ was added, and the resulting solution was reacted under magnetic stirring for 1 h. The initial violet-colored mixture turned into an orange solution, which was treated with activated charcoal for several minutes and filtered on a Celite filter. Concentration under reduced pressure of the filtered solution and addition of Et₂O yielded 66 mg (44% yield) of the title complex as a whitish powder. ¹H NMR (CDCl₃): δ 3.21 (s, 2H, fn-CH), 4.40–4.68 (bm, 4H, CH₂S), 7.17–7.49 (m, 12H, pyr-H_{3,5} and Ph-H), 7.61 (t, 1H, $J = 7.7$ Hz, pyr-H₄). ¹³C NMR (CDCl₃): δ 23.9 (fn-CH), 46.5 (CH₂S), 122.6 (CN), 123.2 (pyr-C_{3,5}), 128.8, 129.8, 132.1, and 133.2 (Ph-C), 138.7 (pyr-C₄), 158.8 (pyr-C_{2,6}). IR (cm⁻¹): 2201 (C≡N). Anal. Calcd for C₂₃H₁₉N₃PdS₂: C, 54.38; H, 3.77; N, 8.27. Found: C, 54.53; H, 3.58; N, 8.37.

The complexes [Pd(η^2 -fn)SNS(1)], [Pd(η^2 -fn)SNS(2)], and [Pd(η^2 -fn)SNS(3)] were synthesized in the same way as [Pd(η^2 -fn)SNS(0)] using the appropriate SNS ligand.

[Pd(η^2 -fn)SNS(1)]: whitish powder, 84% yield. ¹H NMR (CDCl₃): δ 1.46 (m, 12H, CH₂CH₃), 3.16 (s, 2H, fn-CH), 4.47 (q, 12H, $J = 7.1$ Hz, CH₂CH₃ and bs, CH₂S), 5.03 (s, 2H, PhCH₂O), 5.19 (s, 4H, CH₂Opyr), 6.88 (s, 2H, pyr-H_{3,5}), 7.29–7.58 (m, 13H, Ph-H), 7.84 (s, 4H, pyr-H_{3,5}). ¹³C NMR (CDCl₃):

δ 14.6 (CH₃CH₂), 23.9 (fn-CH), 46.5 (CH₂S), 62.9 (CH₃CH₂), 70.4 and 71.1 (CH₂O), 110.0 and 114.9 (pyr-C_{3,5}), 122.5 (CN), 127.9, 129.0, 129.2, 129.3, 132.0, 134.1, 134.8, and 135.5 (Ph-C), 150.7 and 160.0 (pyr-C_{2,6}), 165.0 (C=O), 166.7 (pyr-C₄). IR (cm⁻¹): 2207 (C≡N), 1741 and 1720 (C=O). MALDI-MS: m/z 1041 ([SNS(1)Pd]⁺). Anal. Calcd for C₅₄H₅₁N₅O₁₁PdS₂: C, 58.09; H, 4.60; N, 6.27. Found: C, 58.23; H, 4.31; N, 6.21.

[Pd(η^2 -fn)SNS(2)]: whitish powder, 71% yield. ¹H NMR (CDCl₃): δ 1.45 (m, 24H, CH₂CH₃), 3.11 (s, 2H, fn-CH), 4.46 (q, 12H, $J = 7.1$ Hz, CH₂CH₃, and bs, CH₂S), 5.07 (s, 2H, PhCH₂O), 5.11 (s, 4H, CH₂Opyr), 5.30 (s, 8H, pyrCH₂Opyr), 6.98 (s, 2H, pyr-H_{3,5}), 7.02 (s, 4H, pyr-H_{3,5}), 7.28–7.52 (m, 13H, Ph-H), 7.89 (s, 8H, pyr-H_{3,5}). ¹³C NMR (CDCl₃): δ 14.6 (CH₃CH₂), 23.9 (fn-CH), 46.2 (CH₂S), 62.9 (CH₃CH₂), 69.9 and 71.2 (CH₂O), 108.0, 110.2, and 115.0 (pyr-C_{3,5}), 122.5 (all-CN), 128.0, 128.9, 129.2, 129.3, 131.4, 134.1, 134.8, and 135.7 (Ph-C), 150.8, 157.3, and 159.9 (pyr-C_{2,6}), 164.9 (C=O), 166.6, 166.8, and 166.9 (pyr-C₄). IR (cm⁻¹): 2204 (C≡N), 1740 and 1718 (C=O). MALDI-MS: m/z 1758 ([SNS(2)Pd]⁺). Anal. Calcd for C₉₀H₈₇N₉O₂₃PdS₂: C, 58.96; H, 4.78; N, 6.88. Found: C, 59.23; H, 4.66; N, 6.93.

[Pd(η^2 -fn)SNS(3)]: whitish powder, 90% yield. ¹H NMR (CDCl₃): δ 1.43 (t, 48H, $J = 7.1$ Hz, CH₂CH₃), 3.08 (s, 2H, fn-CH), 4.46 (q, 36H, $J = 7.1$ Hz, CH₂CH₃ and CH₂S), 5.06 (s, 2H, PhCH₂O), 5.10 (s, 4H, CH₂Opyr), 5.21 (s, 8H, pyrCH₂Opyr), 5.32 (s, 16H, pyrCH₂Opyr), 6.97 (s, 2H, pyr-H_{3,5}), 7.01 (s, 4H, pyr-H_{3,5}), 7.10 (s, 8H, pyr-H_{3,5}), 7.33–7.52 (m, 13H, Ph-H), and 7.90 (s, 16H, pyr-H_{3,5}). ¹³C NMR (CDCl₃): δ 14.6 (CH₃CH₂), 24.0 (fn-CH), 46.3 (CH₂S), 62.8 (CH₃CH₂), 69.9, 70.9, and 71.2 (CH₂O), 107.8, 108.0, 110.1, and 114.9 (pyr-C_{3,5}), 122.4 (all-CN), 127.9, 129.1, 129.3, 131.4, 134.1, 134.8, and 135.8 (Ph-C), 150.8, 157.3, 157.5, and 159.9 (pyr-C_{2,6}), 164.9 (C=O), 166.6, 166.7, and 166.8 (pyr-C₄). IR (cm⁻¹): 2210 (C≡N), 1744 and 1719 (C=O). MALDI-MS: m/z 3192 ([SNS(3)Pd]⁺). Anal. Calcd for C₁₆₂H₁₅₉N₁₇O₄₇PdS₂: C, 59.56; H, 4.91; N, 7.29. Found: C, 59.66; H, 4.74; N, 7.04.

NMR Measurements. The temperature-dependent ¹H NMR spectra were analyzed using the SWAN program.²⁰

UV–Vis, Kinetic Measurements, and Data Analysis. The kinetics of allyl amination of complexes [Pd(η^3 -allyl)SNS]-SO₃CF₃ were studied by adding known aliquots of piperidine solution to a solution of [Pd(η^3 -allyl)SNS]SO₃CF₃, fn, and the appropriate ligand SNS in the thermostated cell compartment of a PE Lambda 40 spectrophotometer. The reactants were in constant excess over the metal ([Pd]₀ \approx 1 \times 10⁻⁴ mol dm⁻³), and the progress of the reaction was monitored by recording absorbance changes in the range 500–280 nm or at fixed wavelength with time. Mathematical and statistical data analysis was carried out on a personal computer by means of a locally adapted version of Marquardt's algorithm.²¹

Acknowledgment. We wish to thank Dr. R. Seraglia (CNR Padua) for the MALDI-TOF spectra and the Italian Ministero dell'Università e della Ricerca Scientifica for financial support (40%).

OM020391L

(21) Balacco, G. J. *Chem. Inf. Comput. Sci.* **1994**, *34*, 1235.

(22) Marquardt, D. W. *SIAM J. App. Math.* **1963**, *11*, 431.